

TEMPORAL PROFILE OF THE LCLS PHOTOCATHODE ULTRAVIOLET DRIVE LASER TOLERATED BY THE MICROBUNCHING INSTABILITY*

Juhao Wu[†], P. Emma, Z. Huang, C. Limborg, SLAC, Menlo Park, CA 94025, USA
M. Borland, APS, ANL, Argonne, IL 60439, USA

Abstract

The LCLS electron beam generated in the photoinjector is subject to various instabilities in the downstream acceleration and compression. The instability can be initiated by e-beam density modulation at birth. In this paper, we prescribe the tolerance on the initial e-beam density modulation possibly introduced by the ultraviolet (uv) laser at the cathode. Our study shows that the initial rms density modulation of the e-beam at the photocathode shall be less than 5 % to ensure the FEL lasing and saturation.

Introduction

The success of FEL calls for a high quality e-beam, which is, however, subject to various impedance in the downstream acceleration and compression after being generated from a photocathode. Specifically, the impedance (space charge, wakefield, and CSR) and momentum compaction factor act as an amplifier for initial density and energy modulations. Since the slice emittance and energy spread are extremely small, Landau damping is not effective in suppressing instabilities, which can increase the slice energy spread and emittance, and therefore degrade FEL lasing. FEL operation calls for best achievable beam quality; yet, unnecessarily high quality renders it more susceptible to instabilities described above. To address this quandary, a laser-heater [1] is introduced into the LCLS beamline. The laser-heater is designed to be an adjustable control, which will impose a limited increase on the slice energy spread to the level where FEL lasing is still guaranteed. This ‘procured’ increase is designed to enhance Landau damping such that downstream instabilities can be suppressed. Density and energy modulations can be initiated by shot noise in the e-beam born at the photocathode. Also, temporal modulation on the ultraviolet (uv) laser pulse itself can be transferred to the e-beam at birth. These initial e-beam density or energy modulations can be amplified to affect the FEL lasing. Hence, we study the tolerance of the e-beam density modulations at birth.

Simulation details and results

In our study, we take the nominal LCLS accelerator system setup including the laser-heater, with parameters in Table 1. The laser-heater is to be installed where the e-beam $E = 135$ MeV. Parameters for the laser-heater are in Table 2. We use a total temporal compression factor of 30. Hence, if we require the rms slice relative energy spread

Table 1: Main parameters for the LCLS FEL.

Parameter	Symbol	Value
electron energy	γmc^2	14.1 GeV
bunch charge	Q	1 nC
bunch current	I_f	3.4 kA
transverse norm. emittance	$\varepsilon_{x,y}^n$	1 μm
average beta function	$\beta_{x,y}$	25 m
undulator period	λ_u	0.03 m
undulator field	B	1.3 T
undulator parameter	K	3.64
undulator length	L_u	130 m
FEL wavelength	λ_r	1.5 \AA
FEL parameter	ρ	4.8×10^{-4}

Table 2: Main parameters for the LCLS laser-heater.

Parameter	Symbol	Value
electron energy	$\gamma_0 mc^2$	135 MeV
average beta function	$\beta_{x,y}$	10 m
transverse rms beam size	$\sigma_{x,y}$	190 μm
undulator period	λ_u	0.05 m
undulator field	B	0.33 T
undulator parameter	K	1.56
undulator length	L_u	0.5 m
laser wavelength	λ_L	800 nm
laser rms spot size	σ_r	175 μm
laser peak power	P_L	1.2 MW
Rayleigh range	Z_R	0.6 m
maximum energy modulation	$\Delta\gamma_L(0)mc^2$	80 keV
rms local energy spread	$\sigma_{\gamma_L} mc^2$	40 keV

$\sigma_\delta \approx 1 \times 10^{-4}$ at $E = 14.1$ GeV, then the laser-heater should give a maximum rms slice energy spread $\sigma_E \approx 47$ keV, assuming the conservation of the longitudinal phase space area. This slice σ_E then determines the Landau damping strength to suppress instabilities. The laser-heater introduces energy modulation at wavelength of 800 nm; however, the chicane provides an R_{52} large enough, so that the laser-heater induced energy modulation is washed out by the second half of the chicane. Hence, the laser-heater induced energy modulation becomes purely slice energy spread; and will not be converted into density modulation.

In our study, we take two approaches. In the first one, we introduce a density modulation at the injector end ($E = 135$ MeV). In the second one, we introduce a density modulation in the e-beam at birth. Details are the follows.

Approach I: we take a PARMELA output distribution at

* Work supported by the U.S. Department of Energy under Contract No. DE-AC03-76SF00515, and No. W-31-109-ENG-38.

[†] jhwu@SLAC.Stanford.EDU

Table 3: Summary of the parameters and results for the microbunching and final slice relative energy spread.

		Approach I						Approach II			
Energy modulation amplitude at cathode	keV	0						0			
Density modulation amplitude at cathode	%	0						8			
Energy modulation amplitude at injector end	keV	0						0.3	3.1	1.2	
Density modulation amplitude at injector end	%	1			4			0.7	1.0	1.3	
Density modulation wavelength	μm	15	30	60	100	150	200	150	50	150	300
Final slice rms relative energy spread at 14 GeV	10^{-4}	0.9	0.9	0.9	0.8	0.9	0.8	1.0	1.1	1.0	1.0

the injector end at 135 MeV with 200,000 macroparticles with no density or energy modulation. We then find out the longitudinal momentum correlation, the local slice energy spread correlation, the transverse emittance and its correlations. Preserving all these information, we then use Halton-sequence ‘quiet-start’ in 6-D to generate 2 million macroparticles and superimpose an initial $\pm 1\%$ density modulation with 6 different wavelengths. We also did one simulation with an initial $\pm 4\%$ density modulation to check linearity. Here, the laser-heater introduces a slice $\sigma_E \approx 40$ keV with results in Table 3. The slice σ_δ is the average of the central 20 μm portion of the e-beam. Each slice is 0.5 μm to match the FEL slippage distance.

Approach II: here, 1 million macroparticles with an initial $\pm 8\%$ density modulation for 3 different wavelengths are generated at the cathode. They are tracked through the photoinjector via ASTRA code [2], and the rest of accelerator system via Elegant code [3]. Here, the laser-heater introduces the maximum allowable slice $\sigma_E = 47$ keV, with results in Table 3. In contrast to the e-beam in approach I, there exists energy modulation at injector end.

To further reduce the noise effect, a high pass filter is introduced in the Elegant simulation [1]. In our study, we simulate a single frequency modulation. When the gain is high enough, the instability can run into the nonlinear regime, where harmonics will show up. To account for this, we set the high pass filter slightly higher than the second harmonic. In doing so, modulation with frequencies higher than the second harmonic is filtered out, however, modulations with frequencies between the second harmonic (included) and the original frequency are preserved.

To illustrate how the beam instability degrades the longitudinal phase space, and how effectively the laser-heater can Landau damp the instability, here we show a typical comparison between a matched laser-heater and no laser-heater. (A matched laser-heater is a device where the transverse laser beam size is approximately equal to that of the e-beam.) Figure 1 shows the longitudinal phase space at the undulator entrance without laser-heater, and Fig. 2 with a matched laser-heater. These figures are the approach II simulation at wavelength $\lambda = 150 \mu\text{m}$. In Fig. 1, we find a very large final energy modulation at period about $150 \mu\text{m}/30 = 5 \mu\text{m}$. This indicates that the initial 150 μm density modulation leads to a large energy modulation after the 30 times compression. Besides this initial 150

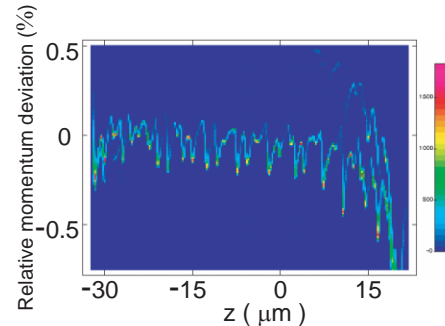


Figure 1: (Color) Longitudinal phase space at the undulator entrance. An initial $\pm 8\%$ density modulation at 150 μm in Approach II simulation without laser-heater.

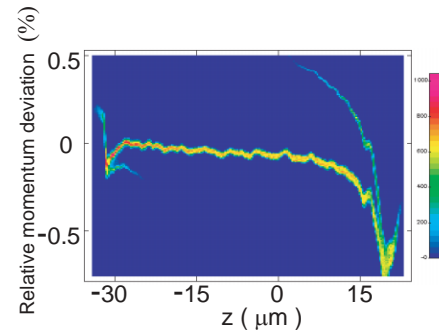


Figure 2: (Color) Longitudinal phase space at the undulator entrance. An initial $\pm 8\%$ density modulation at 150 μm in Approach II simulation with a matched laser-heater.

μm modulation, the second harmonic is also clearly shown. This indicates that the system has evolved into the nonlinear regime. With a matched laser-heater, the results differ significantly as in Fig. 2. The effectiveness of the matched laser-heater is seen in the greatly reduced amplitude of energy modulation at the 5 μm period. The quantity which will affect the FEL lasing is the slice energy spread within the slippage length. We then plot, in Fig. 3, the slice σ_δ along the e-beam. The matched laser-heater clearly limits $\sigma_\delta < 1.0 \times 10^{-4}$ at the central portion of the e-beam. In

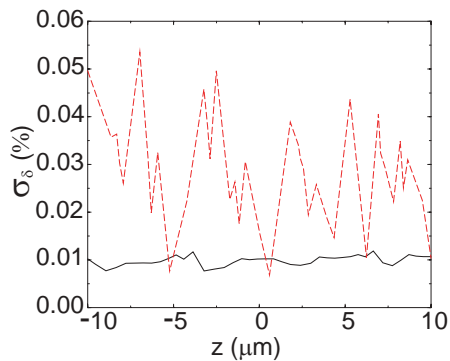


Figure 3: (Color) Slice σ_δ at the undulator entrance. An initial $\pm 8\%$ density modulation at $150 \mu\text{m}$ in Approach II simulation. Solid curve: a matched laser-heater; and dashed curve: no laser-heater.

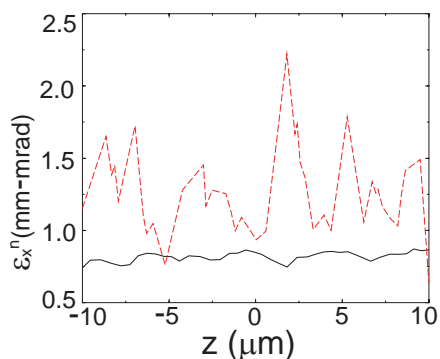


Figure 4: (Color) Slice ϵ_x^n at the undulator entrance. An initial $\pm 8\%$ density modulation at $150 \mu\text{m}$ in Approach II simulation. Solid curve: a matched laser-heater; and dashed curve: no laser-heater.

contrast, without laser-heater, σ_δ is much too high. Similarly, for the slice normalized x emittance ϵ_x^n , Figure 4 shows that $\epsilon_x^n < 1$ mm-mrad along this central portion of the e-beam with a matched laser-heater. Without laser-heater, the ϵ_x^n is much larger. For the other wavelength, the conclusion is the same.

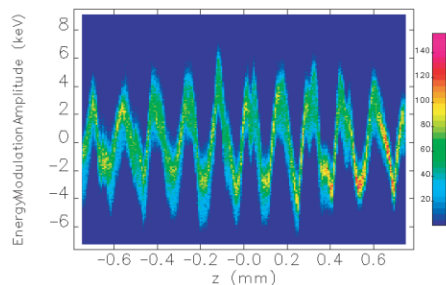


Figure 5: (Color) Energy modulation along the bunch at the injector end, but prior to the laser-heater. An initial $\pm 8\%$ density modulation at $150 \mu\text{m}$ in Approach II simulation.

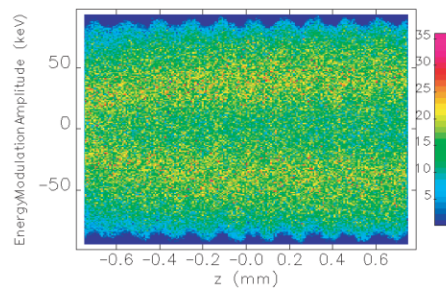


Figure 6: (Color) Energy modulation along the bunch at the end of a matched laser-heater. An initial $\pm 8\%$ density modulation at $150 \mu\text{m}$ in Approach II simulation.

Discussion and conclusion

It is important to clarify the distinction between approach I and II. Table 3 shows that the initial $\pm 8\%$ density modulation is reduced after the injector. However the known space-charge oscillation results in an accumulated energy modulation. This residual energy modulation can be reconverted back into a density modulation without the laser-heater. A matched laser-heater induces a slice $\sigma_E \approx 40$ keV to enhance Landau damping and smear out the residual energy modulation. To demonstrate this, in Figs. 5 and 6, we chose the $150 \mu\text{m}$ wavelength example in approach II. It is seen in Table 3 that the density modulation is reduced to the $\pm 1\%$ level and the accumulated energy modulation has increased from zero to ± 3 keV. Relative to the 3 keV slice σ_E , this is a 100% modulation as in Fig. 5. By contrast, Fig. 6 shows that with a matched laser-heater, this accumulated energy modulation is only about 7% of the slice σ_E . Landau damping suppresses the reconversion of this residual energy modulation back to a density modulation in BC1, and suppresses the instability effectively.

In our study, all the simulations are done for density modulation at a specified frequency. The results show that without the laser-heater, the gain of the microbunching is too high to make FEL lasing possible. Use of a matched laser-heater indicates that the FEL requirement of slice $\sigma_\delta < 10^{-4}$ and slice $\epsilon_x^n < 1$ mm-mrad can be met with a peak-to-peak e-beam density modulation as much as $\pm 8\%$ at the photocathode. This we interpret as the maximum density modulation tolerance at birth. From the $\pm 8\%$ modulation for all wavelengths and a relative insensitivity to wavelength in $50 \mu\text{m}$ to $300 \mu\text{m}$ interval, we determine this maximum tolerance to be a 5% rms value. Because the e-beam density modulation is driven by the uv laser pulse. This is therefore the upper limit to the rms noise on the temporal profile of the uv laser pulse.

References

- [1] Z. Huang *et al.*, PRST AB, **7**, 074401 (2004).
- [2] C. Limborg *et al.*, EPAC'04, 2004.
- [3] M. Borland, ANL/APS Report No. LS-287, 2000.